Gauge-invariant rotor Hamiltonian from dual variables of 3D $U(1)$ gauge theory

Judah F. Unmuth-Yockey*

Department of Physics, Syracuse University, Syracuse, New York 13244, USA

(Received 3 December 2018; published 9 April 2019)

We present a tensor formulation for free compact electrodynamics in three Euclidean dimensions and use this formulation to construct a quantum Hamiltonian in the continuous-time limit. Gauge-invariance is maintained at every step and ultimately the gauge fields are integrated out, removing all initial gauge freedom. The resulting Hamiltonian can be written as a rotor model. The energy eigenvalues for this Hamiltonian are computed using the tensor renormalization group, and are compared with perturbation theory. We find good agreement between the calculations, demonstrating a smooth passage from the statistical lattice Lagrangian description to the quantum Hamiltonian description.

DOI: 10.1103/PhysRevD.99.074502

I. INTRODUCTION

In the last decade there has been an effort in the development and application of tensor real-space renormalization group methods for the lattice (for instance [1–6]) or TRG. The TRG allows one to carry out genuine real-space renormalization group steps exactly as Kadanoff [7] and Wilson [8] prescribed, and many approximation schemes have been invented within this framework. These methods present a number of advantages over traditional sampling (Monte Carlo or MC) methods, most notably an indifference to the sign problem [9], and when translation invariance holds the infinite-volume limit is easily achieved. However, it has been difficult to construct efficient TRG methods in spacetime dimensions larger than two.

An additional pleasant feature of the TRG formalism is the typical reformulation of the model of interest in terms of discrete fields, which are easier to accommodate computationally. These discrete fields are convenient for re-writing the partition function as a contraction over local tensors which, when done exactly, reproduces the partition function. This is a tensor network representation, or tensor formulation, of the model. These discrete variables have not only been useful in tensor formulations, but also in sampling methods [10,11]. This discreteness has been found to be advantageous for making contact with quantum computation, specifically analogue quantum computing [12–14]. There, one works with atomic species whose Hamiltonian descriptions are in terms of creation and annihilation operators and whose occupations are discrete [15]. The discrete nature of the tensor indices comes about from the reformulation of the model using dual variables, in this case, from the compact nature of the original variables. Once the model has been written in terms of a local tensor whose indices are these discrete dual variables, this tensor formulation allows one to identify a transfer matrix for the physical degrees of freedom (d.o.f.) as simply a contraction of these local tensors along a timeslice. Tensor formulations then elucidate the relationships between different d.o.f. through their nonzero elements, and seeing these relationships helps construct models for the discrete d.o.f. used in quantum computation, e.g., quantum simulation.

Here we use a particular TRG scheme, the higher-order tensor renormalization group (HOTRG) [2], to study the continuous-time behavior of three-dimensional compact free electrodynamics. By reformulating this model in terms of its dual variables, we are able to rewrite the partition function as a spin-model while removing the initial gauge freedom from the final result. This is consistent with Ref. [16] where a gauge-spin duality for three dimensional Abelian models is worked out in detail. Here, the duality between the $U(1)$ gauge theory and its corresponding spin system is used as a path to the continuous-time Hamiltonian formulation for this model.

A similar approach to constructing spin systems from gauge models (although accomplished completely in the Hamiltonian formulation) for general $SU(N)$ groups was considered in Ref. [17]. The Hamiltonian constructed there reduce to the Hamiltonian constructed here for the case of the gauge group $U(1)$. In Ref. [18], duality also plays a similar role in restricting the physical state space and enforcing Gauss's law.

*jfunmuthyockey@gmail.com

Here the duality transformation is carried out entirely in the original statistical mechanics model, treating Euclidean time identically to space. We then take the continuous-time limit of this formulation as worked-out in Refs. [19,20]. The integer dual variables on the fully discrete lattice theory can be interpreted as the z-component angular momentum quantum numbers in the continuous-time limit, and we construct a rotor Hamiltonian for this model.

Because the original gauge model can be recast as a spin model, the tensor formulation of this model is simplified and it can be written in terms of a single local tensor. This allows the use of approximate tensor renormalization group methods to coarse grain. Using the HOTRG, we are able to coarse grain the system, and construct an approximate transfer matrix in terms of the physical d.o.f., and by tuning the bare parameters we can study the continuous-time limit. We are then able to diagonalize this approximate transfer matrix and obtain the approximate energy eigenvalues for the continuous-time limit Hamiltonian. Comparison between numerical and perturbative analytical results shows good agreement.

The rest of the paper is organized as follows: In Sec. II we introduce the model and reformulate it in terms of its dual variables. Then using the dual variables we rewrite the partition function as a sum of local tensor contractions. We compare with Monte Carlo to check the validity of the description. In Sec. III we use the tensor formulation of the model to construct a transfer matrix and take the continuous-time limit. In this limit we extract a quantum Hamiltonian from the transfer matrix and interpret the Hamiltonian as a rotor model. With this Hamiltonian we compare calculations of its energy eigenvalues using the HOTRG with calculations done with perturbation theory and find good agreement. Finally in Sec. IV we give concluding remarks about the work and possible future directions.

II. DUAL VARIABLES OF 3D $U(1)$ GAUGE THEORY

The starting action for $U(1)$ lattice gauge theory in three Euclidean dimensions on a cubic lattice of spatial dimensions $N_x \times N_y = N_s$, and temporal extent N_τ, is

$$S = -\beta \sum_x \sum_{\mu>\nu=1}^{3} \Re[U_{x,\mu} U_{x+\hat{\mu},\nu} U^\dagger_{x+\hat{\nu},\mu} U^\dagger_{x,\nu}] \tag{1}$$

$$= -\beta \sum_{x,\mu\nu} \cos(A_{x,\mu} + A_{x+\hat{\mu},\nu} - A_{x+\hat{\nu},\mu} - A_{x,\nu}) \tag{2}$$

$$= -\beta \sum_{x,\mu\nu} \cos(F_{x,\mu\nu}), \tag{3}$$

where x denotes the lattice site location, and μ, ν denote the direction so that $x + \hat{\mu}$ denotes a unit step in the $\hat{\mu}$ direction. The gauge fields, $U_{x,\mu} = e^{iA_{x,\mu}}$, are associated with the links of the lattice, and $\beta = 1/g^2$ with g the gauge coupling. The action consists of a product of gauge fields around an elementary square (plaquette) of the lattice, reproducing the curl of the vector potential in the continuum. The partition function is

$$Z = \int \mathcal{D}[A_{x,\mu}] e^{-S}, \tag{4}$$

where the vector potential is periodic $A_{x,\mu} \in [0, 2\pi]$.

The Boltzmann weight can be expanded using the conjugate Fourier variables as one does in the tensor formulation, or duality transformation [4,16],

$$e^{-S} = \prod_{x,\mu\nu} \sum_{n_{x,\mu\nu}=-\infty}^{\infty} I_{n_{x,\mu\nu}}(\beta) e^{i n_{x,\mu\nu} F_{x,\mu\nu}}. \tag{5}$$

Here there is an antisymmetric $n_{x,\mu\nu}$ field, where $n_{x,\mu\nu}$ is an integer associated with each plaquette on the lattice, and the $I_n(z)$ are the modified Bessel functions. They are symmetric under $n \to -n$ for $z \geq 0$. Each link is shared by four plaquettes in three dimensions. The integration over the vector potential now factorizes and we find for each link,

$$\int \frac{dA_{x,\mu}}{2\pi} e^{iA_{x,\mu}(n_1+n_2-n_3-n_4)} = \delta_{n_1+n_2-n_3-n_4,0}, \tag{6}$$

where the four ns correspond to the four plaquettes in the coboundary of the link. The partition function can now be written

$$Z = \sum_{\{n\}} \left(\prod_{x,\mu\nu} I_{n_{x,\mu\nu}}(\beta) \right) \left(\prod_{x,\mu} \delta_{\Delta_\nu n_{x,\nu\mu},0} \right), \tag{7}$$

where Δ_ν is the lattice forward derivative, $\Delta_\nu f_x = f_{x+\hat{\nu}} - f_x$.

The $n_{x,\mu\nu}$ variables are associated with plaquettes of the lattice, and the Kronecker deltas enforce relations between ns associated with different spacetime slices. These relations are just Maxwell's equations, where $n_{x,\mu\nu}$ are the discrete components of the electric and magnetic fields.

At this point the Kronecker deltas enforcing a zero-divergence constraint can be solved identically using the curl [16],

$$\Delta_\mu n_{x,\mu\nu} = 0 \Rightarrow n_{x,\mu\nu} = \epsilon_{\mu\nu\rho} \Delta_\rho m_{x^*}. \tag{8}$$

The ms are located at the centers of the cubes of the original lattice (the dual lattice sites, x^*) which is necessary in order to simultaneously satisfy all the surrounding constraints associated with the links. Inserting this into the partition function we get,

$$Z = \sum_{\{m\}} \left(\prod_{x,\mu\nu} I_{\epsilon_{\mu\nu\rho}\Delta_\rho m_{x^*}}(\beta) \right). \tag{9}$$

At this point it is convenient to switch to the dual lattice. At the center of each cube we assign a site, and for each plaquette we assign a link connecting two dual sites. The partition function is essentially identical,

$$Z = \sum_{\{m\}} \left(\prod_{x^*,\mu} I_{\Delta_\mu m_{x^*}}(\beta) \right) \tag{10}$$

except the sites are the dual sites, and the product is over dual links. We will drop the asterisk from now on and only work in the dual. This can be split into dual time and space links,

$$Z = \sum_{\{m\}} \left(\prod_{x,\tau} I_{m-m'}(\beta_s) \right) \left(\prod_{x,i} I_{m-m'}(\beta_\tau) \right). \tag{11}$$

We have relaxed the notation surrounding the ms since the Bessel functions are symmetric in their order, and their order is the difference between m values at adjacent sites. The partition function in Eq. (11) is similar to the dual partition function for the Abelian Higgs model in Ref. [14], although they are in two different spacetime dimensions and one model includes scalar matter. This similarity is due to the fact that both models have discrete fields associated with their dual links, and these fields are constrained to be divergenceless at either the sites (in the 2D case), or the links (in the 3D case). Notice the temporal coupling is associated with the dual spatial links and the spatial coupling is associated with the dual temporal links.

In arriving at this final form of the partition function, gauge invariance is maintained at each step until the gauge fields are completely integrated out, arriving at a model with no remaining gauge freedom. In fact, even if the sum over n in Eq. (5) is truncated, the local invariance is unaffected and one is simply left with an effective model with the same symmetries. This is because the expansion is in terms of the gauge-invariant quantity $F_{\mu\nu}$, and so if one were to make a gauge transformation in the truncated form of Eq. (5), the expansion would be unaffected. After Eq. (5) all configurations of the gauge field are integrated over.

A. Tensor formulation of the model

The dual variables from the previous section can be used straightforwardly to construct a local tensor from which the entire partition function can be reconstructed. Similar tensor constructions as well as dual-variable formulations for other models can be found in Refs. [4,14,16,21]. This formulation is not unique, and a tensor formulation for 3D $U(1)$ was put forth in Ref. [4]. However, the U(1) gauge tensor constructed in Ref. [4] has indices, which correspond to different directions in spacetime, that lack symmetry under transposition. In contrast, the tensor constructed here is symmetric under any transposition of its indices. To form a tensor we first notice that the partition function from Eq. (11) describes a theory of integer fields located on the sites of a lattice with nearest neighbor interactions. To isolate the integer fields on the sites, we interpret the Bessel function weights as matrices in their m indices, and factorize them as,

$$I_{m-m'}(\beta) \equiv A_{mm'}(\beta) = \sum_{\alpha=-\infty}^{\infty} L_{m\alpha}(\beta) L^T_{\alpha m'}(\beta). \tag{12}$$

This decomposition is not unique, and is simply the matrix square root. This decouples the integer fields at the sites from their nearest neighbor interaction, and replaces it with an intermediate sum over states. To form a local tensor we define,

$$T_{\alpha\beta\gamma\delta\lambda\sigma} = \sum_{m=-\infty}^{\infty} L_{m\alpha} L_{m\beta} L_{m\gamma} L_{m\delta} L_{m\lambda} L_{m\sigma} \tag{13}$$

which is a function of both the spatial and temporal gauge couplings. The symmetry mentioned above corresponding to the symmetry in tensor indices is completely manifest in Eq. (13). An illustration of this tensor can be seen in Fig. 1. Note that contracting the tensor indices—with each index representing a direction in spacetime—in the shape of the cubic lattice reconstructs the partition function exactly, since through each contraction the Bessel function weights are reconstructed. Therefore one is to think of each Greek

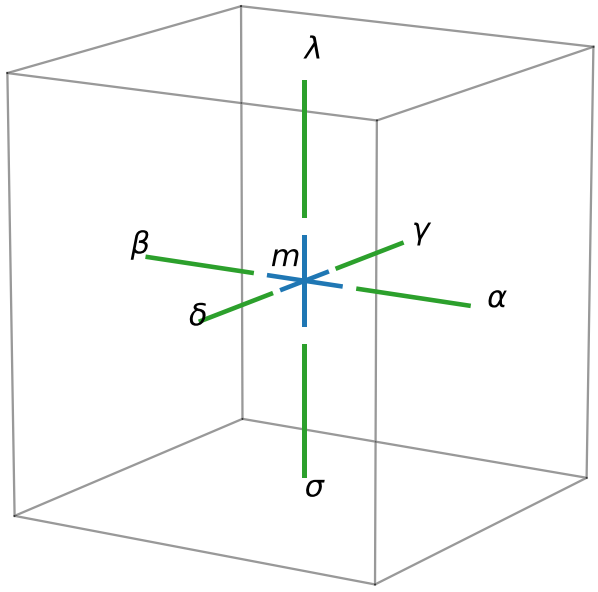

FIG. 1. An illustration of the fundamental local tensor as defined in Eq. (13). Here it is drawn inside of a basic cell of the original lattice, and a blue cross at the center shows the dual site associated with this cell.

index in Eq. (13) as being associated with one of the six directions of a cubic lattice.

In order to check the validity of the tensor formulation presented here, we compared calculations of the average action per plaquette between Monte Carlo and the HOTRG,

$$\langle S \rangle = -\frac{\beta}{3V}\frac{\partial \ln(Z)}{\partial \beta}, \tag{14}$$

where V is the spacetime volume. The Monte Carlo calculations implemented the heat bath algorithm on the weights from Eq. (11). These calculations were compared with Monte Carlo calculations done in the original field variables from Eq. (4). A comparison between Monte Carlo calculations and the HOTRG can be seen in Fig. 2. The HOTRG data was extracted from the numerical derivative with respect to β of $\ln(Z)$, which is straight forward to calculate using the HOTRG. The error bars on the HOTRG data were calculated using three different final bond dimensions: 15, 17, and 19; however, these calculations were done by restricting the bond dimension to three states in the initial tensor.

An initial five state truncation was tested and found not to make a noticeable difference leading us to believe that the final truncation is responsible for most of the information loss. The three state truncation allows for weights up to order $n_{x,\mu\nu} = |2|$ in the partition function. With weights up to this order, we can compare with Monte Carlo, as well as strong and weak coupling expansions, up to $\beta \simeq 4$ and find good agreement. In order to compare with even larger values of β one must keep more initial states in the initial tensor. We used the largest difference in the average action between the three data sets to estimate the error and assumed that this largest difference was a good approximation for the error for all points, with the addition of the error from the numerical derivative. Overall we find good agreement between the two methods, which lends support to the validity of the tensor formulation and calculations.

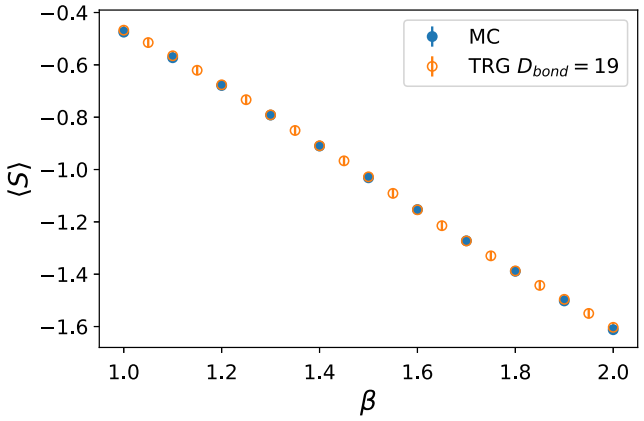

FIG. 2. A comparison between Monte Carlo and HOTRG calculations of the average action per plaquette for a 16^3 lattice. Here an initial bond dimension, D_{bond}, of three was used, and a final D_{bond} of 19. The error for the HOTRG was estimated from the largest difference in three different bond dimensions: 15, 17, and 19. The Monte Carlo calculation averaged over 10 000 configurations and the errors were estimated through jack-knife binning.

III. CONTINUOUS-TIME LIMIT

Using the tensor formulation of the model, we can construct a transfer matrix. Similar approaches to the continuous-time limit, and a transfer matrix construction were put forward in Refs. [12–14,16,19,22]. The construction of the transfer matrix is accomplished by contracting local tensors together along a time-slice. Using periodic boundary conditions, this leaves only tensor indices in the positive and negative time directions. This construction can be seen in Fig. 3. In the figure, the tensor contractions have been drawn to represent the ideal case; however, in practice one must truncate and approximate the local basis using some approximation scheme. In numerical calculations here we used the HOTRG.

The essence of the HOTRG is that one attempts to approximate a tensor with another tensor with smaller dimensional indices, but that has a similar norm. The HOTRG algorithm keeps linear combinations of states from the original tensor such that the norm of the difference between the final tensor and the approximate tensor is minimized [2]. This is the sense in which a tensor analog for the singular value decomposition is used. In practice, it has been found that the HOTRG algorithm picks states that lead to a good approximation of the transfer matrix [12,13,21], while the HOTRG does not necessarily attempt to optimize in this respect.

In order to build an approximate transfer matrix from the fundamental tensor, we contract the initial tensor with itself along a single, say the x, direction and truncate in the orthogonal directions. This allows the x direction to be contracted exactly. The y and τ directions are truncated using the HOTRG procedure. An illustration of this process

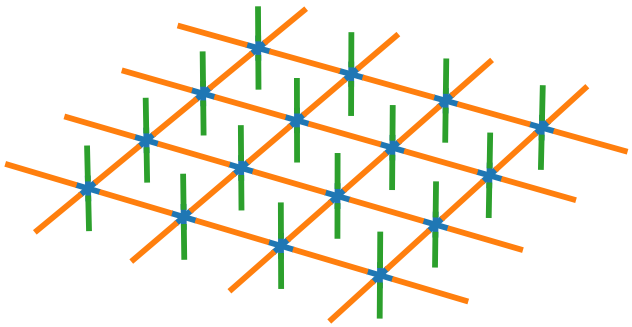

FIG. 3. An illustration of the transfer matrix as constructed by local tensors. Each complete A matrix is orange, while each open index is green. The remaining open indices are either pointing forward, or backwards in time. Here it is assumed the lattice continues in both spatial directions.

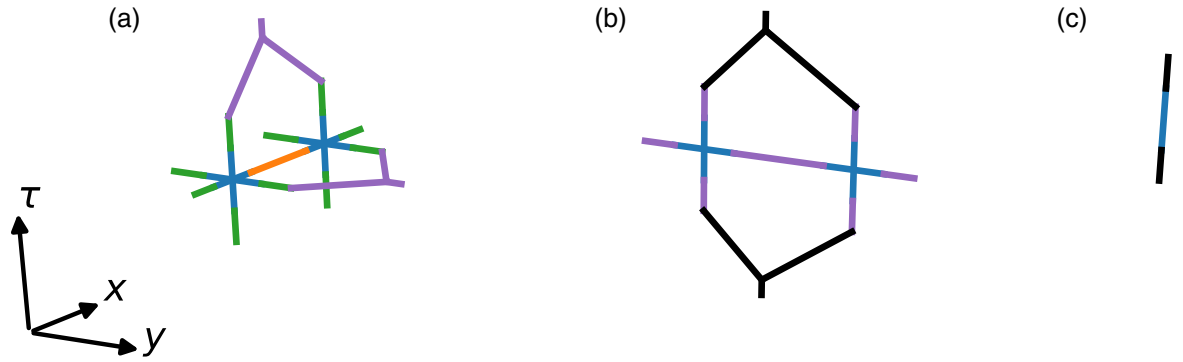

FIG. 4. An illustration of the contractions used to build the approximate transfer matrix. (a) The contraction along the x direction. The original tensor is shown here as in Fig. 1, and an A matrix is shown in orange. Here the initial tensor is contracted with itself along a single direction, and the two perpendicular directions are truncated using the HOTRG algorithm [2], shown in purple (we only show truncation in the positive directions to avoid cluttering the diagram, but in practice one truncates in both positive and negative directions). After the lattice reaches the desired size in the x direction, the final two indices in the x direction are traced over to enforce periodic boundary conditions. (b) The contraction along the y direction. Here the resulting tensor from (a) is contracted with itself along a single direction. The single perpendicular direction (here τ) is truncated using the HOTRG algorithm, shown in black. After reaching the desired size in the y direction, the remaining indices in the y direction are traced over to enforce periodic boundary conditions. (c) The final approximate transfer matrix with indices only in the positive and negative τ directions.

is shown in Fig. 4(a). After the desired lattice size is achieved in the x direction, the two hanging indices in the positive and negative x directions are contracted to have periodic boundary conditions. The tensor is now a four-index tensor, each index representing the positive and negative directions of the y and τ axes. We then contract this tensor with itself along the y axis and, using the HOTRG, truncate in the τ direction. This step is shown in Fig. 4(b). When the desired lattice size in the y direction is achieved, we contract the two hanging indices in the positive and negative y directions to enforce period boundary conditions. The final two-index tensor is the approximate transfer matrix whose only two remaining indices point in the positive and negative τ directions. A graphic of this final matrix can be seen in Fig. 4(c).

We would now like to identify the matrix elements of the transfer matrix. Hereinafter we will work with normalized Bessel functions, $t_n(z) \equiv I_n(z)/I_0(z)$, unless otherwise mentioned. The t_n have the following behavior for large and small arguments,

$$t_n(z) \simeq 1 - \frac{n^2}{2z} + \mathcal{O}(z^{-2}) \quad \text{for } z \to \infty \tag{15}$$

$$t_n(z) \simeq \frac{z^n}{2} + \mathcal{O}(z^{n+2}) \quad \text{for } z \to 0. \tag{16}$$

To identify the matrix elements of the transfer matrix we rewrite the action of the model in a slightly different way than before as [23]

$$S = -\sum_t L(t) \tag{17}$$

with

$$\begin{aligned} L(t) = &\frac{1}{2}\sum_{\langle ij\rangle} \ln t_{m_i(t)-m_j(t)}(\beta_\tau) \\ &+ \frac{1}{2}\sum_{\langle ij\rangle} \ln t_{m_i(t+1)-m_j(t+1)}(\beta_\tau) \\ &+ \sum_i \ln t_{m_i(t)-m_i(t+1)}(\beta_s). \end{aligned} \tag{18}$$

Here the sums, $\sum_{\langle ij\rangle}$ and $\sum_i$ are over nearest neighbor pairs, and all sites, respectively, and the sum $\sum_t$ is over all time slices. This form is useful since the action has now been written as a sum of terms associated with different time slices. Each of these different time-slice terms shares a collection of common m variables with two other terms in the sum. The m variables associated with time slice t are shared and contracted with the m variables on the previous time slice, $t-1$, and the next time slice, $t+1$. Now the partition function can be written,

$$Z = \mathcal{C}\sum_{\{m\}} e^{-S} \tag{19}$$

$$= \mathcal{C}\left(\prod_t \sum_{\{m(t)\}}\right)\left(\prod_t (e^L)_{\{m(t)\}\{m(t+1)\}}\right) \tag{20}$$

$$= \mathcal{C}\mathrm{Tr}\left[\prod_t \mathbb{T}\right]. \tag{21}$$

with $\mathcal{C} = (I_0(\beta_s))^{N_s N_\tau}(I_0(\beta_\tau))^{2N_s N_\tau}$. Here $\{m(t)\}$ denotes the product state of m variables along a time slice t.

Note how in the second product in Eq. (20) over t, each $\{m(t)\}$ appears twice just as matrix indices should. Then the partition function is written as a product of transfer matrices, $\mathbb{T}$, each of which is associated with a time slice, and whose indices are the m variables which are traced over.

First consider the diagonal entries of the transfer matrix. In that case we find

$$L(t) = \sum_{\langle ij \rangle} \ln t_{m_i - m_j}(\beta_\tau). \tag{22}$$

Next, consider a single change of either ± 1 in an m variable between two time slices,

$$L(t) = \frac{1}{2}\sum_{\langle ij \rangle} \ln t_{m_i(t)-m_j(t)}(\beta_\tau) + \frac{1}{2}\sum_{\langle ij \rangle} \ln t_{m_i(t+1)-m_j(t+1)}(\beta_\tau) + \ln t_1(\beta_s). \tag{23}$$

This is the first off-diagonal contribution. One then proceeds systematically through all possible changes in the ms to identify the matrix elements.

In order to relate this model to a quantum Hamiltonian in two spatial dimensions we must find a limit for this transfer matrix where,

$$\mathbb{T} \simeq \mathbf{1} - aH + \ldots \tag{24}$$

with a the temporal lattice spacing, and H a Hamiltonian. This is a limit where the temporal lattice spacing becomes small, and the time direction resembles continuous evolution. To take this continuous-time limit we imagine forcing the temporal couplings to be very strong so to force uniformity in the time direction and simultaneously we make the temporal lattice spacing very small to approach continuity. To that end we take $\beta_\tau \to \infty$, and $\beta_s \to 0$, and the temporal lattice spacing, $a \to 0$ such that

$$U \equiv \frac{1}{\beta_\tau a}, \quad \text{and} \quad X \equiv \frac{\beta_s}{a} \tag{25}$$

are kept constant, and we keep terms in the expansion of the normalized Bessel functions that are of $\mathcal{O}(\beta_s)$ and $\mathcal{O}(\beta_\tau^{-1})$. Looking at Eq. (22) we see that, to leading order, the diagonal part of the transfer matrix has the form

$$\mathbb{T}_{\text{diag}} = \exp\left[-\frac{1}{2\beta_\tau}\sum_{\langle ij \rangle}(m_i - m_j)^2\right]. \tag{26}$$

While keeping to leading order in β_s, we find for a single change of ± 1 in the ms from Eq. (23),

$$\mathbb{T}_{\text{single flip}} = \frac{\beta_s}{2} \times \exp\left[-\frac{1}{2\beta_\tau}\sum_{\langle ij \rangle}(m_i(t) - m_j(t))^2 - \frac{1}{2\beta_\tau}\sum_{\langle ij \rangle}(m_i(t+1) - m_j(t+1))^2\right]. \tag{27}$$

Keeping more spin-flips means keeping higher orders in β_s. In order to match the form $\mathbb{T} \simeq e^{aH}$ we multiply by 1 such that we introduce a factor of $1/a$ in the exponential in Eq. (26) and out front of Eq. (27), while simultaneously multiplying by a factor of a. We see only the $\mathcal{O}(\beta_s)$ and $\mathcal{O}(1/\beta_\tau)$ terms will survive, and the definitions in Eq. (25) come about.

This gives a transfer matrix that implies a Hamiltonian of the form

$$H = \frac{U}{2}\sum_{\langle ij \rangle}(L_i^z - L_j^z)^2 - X\sum_i U_i^x, \tag{28}$$

with the sum $\langle ij \rangle$ over nearest-neighbor pairs. The operators in this Hamiltonian are defined as follows in the z-component of angular momentum basis, as they are in Refs. [21,22],

$$L^z|m\rangle = m|m\rangle \tag{29}$$

$$U^x = \frac{1}{2}(U^+ + U^-) \tag{30}$$

$$U^\pm|m\rangle = |m \pm 1\rangle. \tag{31}$$

These operators satisfy the commutation relations $[L^z, U^\pm] = \pm U^\pm$, $[U^+, U^-] = 0$. We see the first term favors "aligning" adjacent rotors, while the second term attempts to disorder and scramble the rotors.

A. Calculations of the ground state energy

For small systems it is possible to calculate the approximate energy eigenvalues of Hamiltonian (28) accurately using the HOTRG, and compare with perturbation theory calculations. First we compute the perturbative expansion analytically up to quartic order, and then compute the approximate energy eigenvalues of the Hamiltonian directly from the approximate transfer matrix eigenvalues using the approximate transfer matrix constructed from the HOTRG.

For the perturbation theory we begin by rescaling, and using

$$H_0 = \frac{1}{2}\sum_{\langle ij \rangle}(L_i^z - L_j^z)^2 \tag{32}$$

$$V = -x\sum_i U^x, \tag{33}$$

with $x = X/U = \beta_s\beta_\tau$. We see the ground state for the unperturbed Hamiltonian is infinitely degenerate. We add a term to break this degeneracy, and then remove this contribution at the end if the answer permits. Then,

$$H_0 = \frac{1}{2}\sum_{\langle ij\rangle}(L_i^z - L_j^z)^2 + h\sum_i (L_i^z)^2, \tag{34}$$

which picks out the $m = 0$ state as the ground state for H_0. Note that in the case of spatial open boundary conditions (surrounding the spatial ends of the lattice in the $m = 0$ state) this state is picked out automatically since at the spatial boundary in x we have $(L^z_{N_x,y} - L^z_{N_x+1,y})^2 \to (L^z_{N_x,y})^2$, while at the y spatial boundary we have $(L^z_{x,N_y} - L^z_{x,N_y+1})^2 \to (L^z_{x,N_y})^2$. Then a degeneracy breaking term is not needed since in this case H_0 would be minimized by all rotors in the $m = 0$ state. We can use the perturbative formulas for the nth energy eigenvalue [23],

$$E_n = \varepsilon_0 + x\varepsilon_1 + x^2\varepsilon_2 + \ldots \tag{35}$$

with

$$x\varepsilon_1 = \langle n|V|n\rangle \tag{36}$$

$$x^2\varepsilon_2 = \langle n|VgV|n\rangle \tag{37}$$

$$x^3\varepsilon_3 = \langle n|VgVgV|n\rangle - \langle n|V|n\rangle\langle n|Vg^2V|n\rangle \tag{38}$$

$$\begin{aligned} x^4\varepsilon_4 = {} & \langle n|VgVgVgV|n\rangle - \langle n|VgV|n\rangle\langle n|Vg^2V|n\rangle \\ & + \langle n|V|n\rangle\langle n|V|n\rangle\langle n|Vg^3V|n\rangle \\ & - \langle n|V|n\rangle\langle n|VgVg^2V + Vg^2VgV|n\rangle \\ & \vdots \end{aligned} \tag{39}$$

and $g = (1 - |n\rangle\langle n|)/(\varepsilon_0 - H_0)$ to compute the different energy states.

Consider the perturbative corrections for the ground state energy, i.e., $n = 0$. We will restrict the local Hilbert space to three states, a "spin-1" system, with $m = \pm 1, 0$ possible at each site. Noticing that the perturbation V raises or lowers the angular momentum by one, the first contribution must be at second order. We find,

$$\varepsilon_2 = -\frac{1}{4}N_xN_y. \tag{40}$$

Similarly, the next contribution must be at quartic order,

$$\varepsilon_4 = -\frac{N_xN_y}{16}\left[\frac{(N_xN_y - 5)}{2} + \frac{32}{15}\right] + \frac{1}{32}N_x^2N_y^2. \tag{41}$$

The unperturbed ground state energy, ε_0 is simply zero.

Using the HOTRG to compare, we can explicitly take the continuous-time limit described in the previous section in the local tensor, and perform the tensor contractions as described before to approximate the transfer matrix. We then extrapolate the $\beta_\tau \to \infty$, β_s, $a \to 0$ results to the continuous-time limit. To match with perturbation theory, the initial tensor is restricted to three states, however the final bond dimension varied depending on the spatial volume. The three state truncation used in the HOTRG is valid when $X/U \ll 1$. Because U is relatively large compared to X, it is energetically expensive to excite rotor differences greater than $|1|$, since such an excitation is a factor of four larger. Therefore as the rotors disorder at larger X, the three-state approximation breaks down.

In the continuous-time limit, we expect that if we find the eigenvalues of the transfer matrix, λ_n, they are related to the energy eigenvalues of the Hamiltonian through the relation,

$$\mathbb{T} = e^{-aH}. \tag{42}$$

We conclude that for finite β_τ, in units of U, the energy eigenvalues are given by,

$$E_n = -\beta_\tau \ln(\lambda_n). \tag{43}$$

This is because Eq. (25) dictates that the temporal lattice spacing is inversely proportional to β_τ, and in units of U, $a = 1/\beta_\tau$.

A comparison between calculations of the ground state energy using HOTRG, and using perturbation theory can be seen in Fig. 5. Here the two leading-order contributions are plotted, along with data obtained from the HOTRG calculations extrapolated to the $a \to 0$ limit. We find good agreement between the analytic calculation and the numerical calculation with the HOTRG, indicating that the quantum Hamiltonian does in fact correctly model the $U(1)$ gauge theory with which we started.

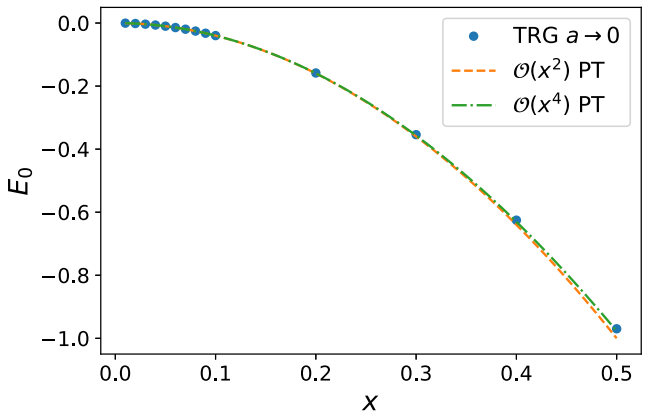

FIG. 5. The ground state energy computed using the HOTRG in the continuous-time limit compared with a perturbation theory (PT) calculation of the same quantity to order x^2 and x^4. This is on a 4×4 spatial lattice.

IV. CONCLUSION

We have presented a tensor formulation for compact 3D free electrodynamics based on a dual variables formulation for the model. In order to check this formulation we compared with Monte Carlo calculations done in the dual variables, and the original variables, and found good agreement between the methods. We used this tensor formulation to extract a quantum Hamiltonian in the continuous-time limit. At each step in this formulation, gauge-invariance is maintained until the gauge fields are integrated over with no gauge freedom remaining. The discrete integer fields from the duality transformation can be interpreted as angular momentum quantum numbers in the continuous-time limit, giving a rotor Hamiltonian description for the model. To check this description, we calculated the approximate ground state energy using the HOTRG and compared it with a perturbative calculation done with the Hamiltonian, and found good agreement.

The Hamiltonian formulation here could be amenable to quantum simulation. Since the final result here has no remaining gauge freedom, there would be no need to enforce Gauss's law by hand in experiment. Instead, one is left with local on-site and nearest neighbor interactions, and one must suppress longer distance interactions, e.g., next-to-nearest neighbor interactions, etc. In addition, optical lattice set-ups tailored for Hamiltonians in this basis have already been put forward [21] and modifications could be straight forward. We are currently investigating the promise of this approach.

In addition, it would be interesting to explore the extent to which the TRG can accurately describe the phase diagram of the model. This would involve a more systematic and careful exploration of thermodynamic quantities, and understanding in detail the role that truncation would play in attempts to accurately calculate observables. This is left as future work.

Finally, one would hope to extend this analysis to non-Abelian gauge groups, however solving for dual variables is difficult in that case. This makes following the steps here in the non-Abelian case unlikely. However, alternate tensor constructions have been put forward in Ref. [4] and could be used if efficient algorithms could be devised.

ACKNOWLEDGMENTS

I would like to thank Yannick Meurice and David Kaplan for stimulating discussions, as well as Jack Laiho and Simon Catterall for discussions and for thoroughly reading the paper. I would like to thank Alexei Bazavov for comparing Monte Carlo values, as well as the referee for their useful comments for improving the article. I would also like to thank the organizers at FermiLab for the workshop "Next steps in quantum science for HEP" where some of this work was done. This work is supported by the U.S. Department of Energy, Office of Science, Office of High Energy Physics, under Award No. DE-SC0009998 and by Grant No. DE-SC0010113.

[1] M. Levin and C. P. Nave, Phys. Rev. Lett. **99**, 120601 (2007).
[2] Z. Y. Xie, J. Chen, M. P. Qin, J. W. Zhu, L. P. Yang, and T. Xiang, Phys. Rev. B **86**, 045139 (2012).
[3] Z. Y. Xie, H. C. Jiang, Q. N. Chen, Z. Y. Weng, and T. Xiang, Phys. Rev. Lett. **103**, 160601 (2009).
[4] Y. Liu, Y. Meurice, M. P. Qin, J. Unmuth-Yockey, T. Xiang, Z. Y. Xie, J. F. Yu, and H. Zou, Phys. Rev. D **88**, 056005 (2013).
[5] G. Evenbly and G. Vidal, Phys. Rev. Lett. **115**, 180405 (2015).
[6] R. Sakai, S. Takeda, and Y. Yoshimura, Prog. Theor. Exp. Phys. **2017**, 063B07 (2017).
[7] L. P. Kadanoff, Phys. Phys. Fiz. **2**, 263 (1966).
[8] K. G. Wilson, Phys. Rev. B **4**, 3174 (1971).
[9] A. Denbleyker, Y. Liu, Y. Meurice, M. P. Qin, T. Xiang, Z. Y. Xie, J. F. Yu, and H. Zou, Phys. Rev. D **89**, 016008 (2014).
[10] C. Gattringer, D. Gschl, and T. Sulejmanpai, Nucl. Phys. **B935**, 344 (2018).
[11] C. Marchis and C. Gattringer, Phys. Rev. D **97**, 034508 (2018).
[12] H. Zou, Y. Liu, C.-Y. Lai, J. Unmuth-Yockey, L.-P. Yang, A. Bazavov, Z. Y. Xie, T. Xiang, S. Chandrasekharan, S.-W. Tsai, and Y. Meurice, Phys. Rev. A **90**, 063603 (2014).
[13] J. Unmuth-Yockey, J. Zhang, P. M. Preiss, L.-P. Yang, S.-W. Tsai, and Y. Meurice, Phys. Rev. A **96**, 023603 (2017).
[14] A. Bazavov, Y. Meurice, S.-W. Tsai, J. Unmuth-Yockey, and J. Zhang, Phys. Rev. D **92**, 076003 (2015).
[15] U.-J. Wiese, Ann. Phys. (Berlin) **525**, 777 (2013).
[16] R. Savit, Rev. Mod. Phys. **52**, 453 (1980).
[17] M. Mathur and T. P. Sreeraj, Phys. Rev. D **94**, 085029 (2016).
[18] D. B. Kaplan and J. R. Stryker, arXiv:1806.08797.
[19] J. Kogut and L. Susskind, Phys. Rev. D **11**, 395 (1975).
[20] E. Fradkin and L. Susskind, Phys. Rev. D **17**, 2637 (1978).
[21] J. Zhang, J. Unmuth-Yockey, J. Zeiher, A. Bazavov, S.-W. Tsai, and Y. Meurice, Phys. Rev. Lett. **121**, 223201 (2018).
[22] J. Unmuth-Yockey, J. Zhang, A. Bazavov, Y. Meurice, and S.-W. Tsai, Phys. Rev. D **98**, 094511 (2018).
[23] J. B. Kogut, Rev. Mod. Phys. **51**, 659 (1979).